VENTILATION OF BACK SPACE OF BUILDING ENCLOSURE SIDING FOR SOLAR HEAT GAIN REDUCTION

Dr. Hiroshi Homma*   Dr. Richard W. Guy**
Member ASHRAE

ABSTRACT

The effect of ventilation in the space between a main wall and an exterior siding is examined with respect to reducing the building's cooling load. The buoyant force of the air in the space is considered as the motive force of air flow and the effect is treated as a problem of simultaneous heat and mass-transfer.

A simulation program of heat and air flows in a wall has been developed using laminar flow theory, and its validity is examined by the comparison of the simulation results with a weather exposed full-scale model test.

The computer simulation shows that the ventilation of air spaces has the potential to reduce the radiative heat gain of both opaque walls and of triple glass windows.

1. INTRODUCTION

A sandwich wall with an insulation layer is a typical wall structure. A siding of small heat capacity is often applied on the exterior side of the insulation sheathing of a sandwich wall. When a back space of a siding is ventilated effectively, the siding can be cooled from its inner surface, and the further heat transmission into the wall body can be reduced effectively. Thus, the siding functions as a compact shading device.

When a siding of small heat capacity absorbs solar radiation, the temperature of the siding rises significantly, and the air in the back space is also heated. The temperature of air in the back space of a light weight metal siding has been found to rise up to 40 degrees C higher than outdoor air as a result of solar radiation in conventional wall structures; in consequence, gravitational or buoyancy forces will have a significant effect in ventilating the back space, with the result that building solar gain may be reduced.

This ventilation effect was examined by using computer simulation of the air movement and heat flow in a space. The results from this simulation were compared with experimental results determined from a full-scale model test.

The ventilation effect of an air space on the thermal performance of various wall and window structures is examined by using the simulation program and the results suggest the potential for passive cooling load reduction by this means.

2. SIMULATION BY NUMERICAL TREATMENT

To analyze the air flow and heat flow in a section of a wall with a ventilated air space, the follwing method was used :

When solar radiation is absorbed in a siding located in front of a wall, this heat is transferred to the air on both sides of the siding. The air at the outer surface is removed mainly by wind. When the air in the back space of the siding is warmer than outside air, buoyancy forces work on the air in the space to make it rise. For this movement, frictional force at wall surface

---

* Associate Professor, Toyohashi University of Technology, Toyohashi,Japan (formerly Assistant Professor, Centre for Building Studies,Concordia Univ.)

** Associate Professor, Center for Building Studies, Concordia University, Montreal, Canada

boundaries and inertia forces combine to oppose the buoyancy force. The air movement in this space stabilizes at a velocity at which the three forces balance.

The heat balance in the space is maintained by heat exchange between the side walls and air, and the heat transportation by the air flow. Consequently, both heat and mass exchange will ultimately dictate the air space temperature. For a balanced condition of air movement and heat flow, heat and force balances must be treated simultaneously (Fig.1). In a laminar flow range, the Newton's theory of frictional force can be applied, and here it is assumed to be applicable. The transition from laminar flow to turbulent flow takes place at Reynold's number equal to 1000[1].

When the width is sufficiently larger than the depth of the air space, the temperature and flow field are assumed to be two-dimensional, and this simulation program is accordingly based on the theory of two dimensional heat and fluid flow [2,3].

An air space is divided into many thin vertical control layers, each of which are parallel to the walls. When the surface temperature on both sides of the air space is higher than the outdoor air, the temperature of the air which flows into the space rises gradually, and the air proceeds upward.

2.1 Balance of Energy

The temperature distribution in the air space is calculated as follows : (Fig. 2). The very thin control layers in the air space are vertically divided into small sections of height h. The heat q_1 (watts) conducted from the next space into the control space under consideration, is a function of the interface area $W \cdot h (m^2)$, distance of centers of the two control spaces d (m), conductivity K (w/m·K) of the air and the temperature difference Δt (K) as given by :

$$q_1 = W \cdot h \cdot K \cdot \frac{\Delta t}{d} \tag{1}$$

where :

W is the width of the space (m).

When the air flow is parallel to the walls, the heat q_2 supplied by the air flow into the space of consideration is :

$$q_2 = Cp \cdot \rho \cdot V \cdot (t_i^{'} - t_i) \cdot W \cdot d \tag{2}$$

where :

$t_i^{'}$ and t_i are, respectively, the temperature of the air which flow into, and out of the i^{th} control space (K);

Cp is the specific heat of the air (Joul/Kg·K);

ρ is the density of the air (Kg/m^3); and

V is the air velocity (m/s).

When the control layers are assigned suffixes i's, and the vertically divided sections are designated by suffixes j's, the heat balance equation in the control space at the i^{th} layer and j^{th} section is :

$$\left(\frac{t_{i-1,j} - t_{i,j}}{\frac{d_{i-1} + d_i}{2}} + \frac{t_{i+1,j} - t_{i,j}}{\frac{d_i + d_{i+1}}{2}} \right) K \cdot W \cdot h + \left(\frac{t_{i,j-1} - t_{i,j}}{\frac{h_{i-1} + h_i}{2}} + \frac{t_{i,j+1} - t_{i,j}}{\frac{h_i + h_{i+1}}{2}} \right) K \cdot W \cdot d_i$$

$$+ Cp \cdot \rho \cdot V_i \, (t_{i-1,j} - t_{i,j}) \, W \cdot d_i = 0 \tag{3}$$

2.2 Heat Flow around Walls

The surface on each of the air space is treated, ideally, as a single layer wall. The equivalent heat conductance is calculated from the series of thermal conductances of every layer for each wall, and the heat transfer by convection and radiation are treated separately on each of the four surfaces of the two walls.

The walls are also divided into 20 sections vertically, in the same manner as the division of the air layers. The heat transfer between a section of a wall surface and the contacting air layer is, subsequently, assumed to take place separately for each of the sections.

The heat exchange between a wall surface and the air layer, which contacts the surface, is performed by conduction of the air. The absorbed heat in the layer is partly conducted to the neighbouring layer, and partly transported by the air movement. Vertical heat transmission through a wall is neglected.

2.3 Balance of Forces

The buoyant pressure which works on the i^{th} control layer is the difference between the gravitational pressure of this control layer, and of the air column of the outside air of the same height. This pressure is a function of the density of the air layer, and the density is expressed as a function of the air layer temperature as :

$$\rho_j = \rho_r \frac{273 + t_r}{273 + t_j}$$

where :

ρ is density in Kg/m^3; and

t is temperature in K of the air.

Suffixes j and r correspond respectively to the air in the layer and to the reference air. When an air layer of height H is vertically divided into n sections, and the temperature and height of each section is expressed by t_j and h_j (j=1 through n), respectively, the gravitational pressures P_1 which is caused by this air layer is the summation of the gravitational pressures of every section; thus :

$$P_1 = \sum_{j=1}^{n} h_j \cdot g \cdot \rho_r \frac{273+t_r}{273+t_j} = g \cdot \rho_r \sum_{j=1}^{n} h_j \frac{273+t_r}{273+t_j}$$

When the air temperature outside of the air space is constant t_o, then the gravitational pressure P_2, caused is :

$$P_2 = g \cdot \rho_r \cdot H \frac{273+t_r}{273+t_o}$$

The difference in the above two pressures P_1 and P_2 is the buoyant pressure P_i, which is the motivational force to move the air in the i^{th} control layer; thus:

$$P_i = P_1 - P_2 = g \cdot \rho_r \left(\sum_{j=1}^{n} h_j \frac{273+t_r}{272+t_j} - H \frac{273+t_r}{273+t_o} \right) \tag{4}$$

When an air mass is accelerated from the still condition out of the air space to a velocity v in the air space, the air mass attains a dynamic force. Some part of the buoyant pressure is converted into dynamic pressure to accelerate the air mass. This dynamic pressure P_d is given by :

$$P_d = \frac{1}{2} \rho_o v^2 \tag{5}$$

where :

ρ_o is the density of the outside air.

The frictional force, which is caused on an air layer by contact with the two neighbouring layers is calculated from Newton's law.

The velocities of $(i-1)^{th}$, i^{th} and $(i+1)^{th}$ layers are expressed by v_{i-1}, v_i and v_{i+1}, respectively; the frictional force F_f, which is caused on the i^{th} layer by the $(i-1)^{th}$ and $(i+1)^{th}$ layers is :

$$F_f = \eta\left(\frac{v_{i-1} - v_i}{\frac{d_{i-1} + d_i}{2}} + \frac{v_i - v_{i+1}}{\frac{d_i + d_{i+1}}{2}}\right) H \cdot W \tag{6}$$

where :

η is the dynamic viscosity of the air ($N \cdot s/m^2$);

d_{i-1}, d_i and d_{i+1} are the thicknesses of $(i-1)^{th}$, i^{th} and $(i+1)^{th}$ layers.

The force F_b, which is caused on the i^{th} layer by the residual of the buoyant pressure subtracted of the velocity pressure, is the product of the horizontal sectional area of the air layer and the residual pressure as :

$$F_b = W \times d_i \times (P_i - P_d)$$

$$= W \cdot d_i \left[g \cdot \rho_r \left(\sum_{j=1}^{n} \frac{273+t_r}{273+t_j} h_j - H \frac{273+t_r}{273+t_o} \right) - \frac{1}{2} \rho_o \cdot v^2 \right] \tag{7}$$

When the motivational force F_b balances with the frictional force F_f, the flow of the i^{th} air layer stabilizes, as (Fig.3) :

$$F_b = F_f \tag{8}$$

The equation of the force balance (8) is established for each layer in the air space.

When a siding is attached on the exterior of a wall, the vertical air passage between the siding and main wall is restricted by the framework. The dynamic force of the air movement is calculated by using the maximum air velocity in the air space. The volumetric flow rate is calculated from the velocity distribution in an air space. The maximum velocity is calculated by dividing the volumetric flow rate by the area of the most restricted part in the air passage, for example the opening at the bottom of the air space in Fig. 1. The dynamic force is assumed to distribute evenly over each air layer.

2.4 Solving Method of Heat and Air Flows in an Air Space

To attain a balanced condition of heat and air flows in an air space, the equations of heat balance and of force balance must be solved simultaneously. The heat balance equation (3) is set for each of the control spaces and wall sections. The force balance equation (8) is set for each control layer.

As the number of unkowns are large, and the equation of force balance is a binomial equation of air velocity, the solution cannot be attained directly from these equations. The balanced condition is sought by successively correcting the velocities and temperatures of the control spaces by optimization techniques, starting from roughly estimated velocity and temperature distributions.

A computer program was developed to process these equations. In this program, an air space is divided into eleven layers, and into twenty equal sections. The thickness of the layers are changed to attain a better simulation result. In the neighbourhood of a wall surface, the temperature and velocity gradients are larger than in the central part of an air space. The thickness of the control layers was set thinner in the periphery than in the centre of an air space (see Figs. 6 & 7).

The computational process required about five hundred repetitions of the correction of temperatures and velocities at every control space. When solar radiation is strong, a strong air flow results, and calculations reach a stable condition with fewer repetitions.

The air velocity calculation showed a character of strong covergence, compared with the stability of the heat balance calculation.

For a typical application, the height of an air space may be the same height to an ordinary floor height of a building, i.e. 2.5 to 3 meters. The ratio of a height to a thickness of an air space then is about 100 for an air space thickness of 25 to 30 mm. Edge effect must be considered at the entrance region for a length of several times that of an air space thickness: however the height of an air space is assumed to be long enough to neglect edge effect for the air flow in a space.

3. EXPERIMENTAL WORK WITH A FULL SCALE MODEL

To verify the simulation of heat and air flows by computation, a full scale model test was carried out under external environmental conditions. This model was placed on the roof of the Centre for Building Studies, Concordia University, Montreal. The model was a box, with a height of 2.5 meters, depth of 3.0 meters and width of 1.2 meters, having a sloping roof. The box was a wood frame structure, with both sides of the framework covered by weatherproof plywood sheets of 19 mm thickness. For this experiment, the spaces between the plywood plates, of depth 89 mm, on the south side wall was insulated with glass wool. The wall consisted of three experimental zones, each of width 406 mm and four control zones of width 406 mm at both sides and between the three experimental zones.

The siding used was aluminum plate, having a thichness of 0.3 mm, coated on both sides with dark brown paint. Each plate had a width of 406 mm and had three grooves of width 20 mm and depth 15 mm at an equal space along its length.

These plates were attached on the south wall with the grooves arranged vertically. The framework to attach the siding were rectangle timbers of 19 mm by 28 mm each, directly attached at the top and bottom wall surface. The height distance of the top and bottom frames was 2.40 meters. Small openings were arranged on the frame of two experimental zones. The openings for zone one were twelve holes of diameter 15mm; the openings for zone two were fifteen holes of diameter 6.35mm. These opening areas correspond to 19% and 4% respectively, of the sectional areas of the air passages. The perimeter of zone three was carefully sealed with synthetic sealant.

On the vertical center line of each experimental zone, temperature sensors were arranged at the middle height and 711mm above and beneath the middle height. Temperature sensors were also arranged on the back surfaces of the siding and in air spaces 5 and 14mm from the surface of the main wall.

For this temperature measurement, copper-constantan thermocouples of diameter 0.3 mm were used. Surface temperatures were monitored by flattened wires extending for about 50mm from the temperature-sensing junctions.

The radiative energy incidence was not measured in this test; instead, the radiative incidence was calculated using the measured temperatures from the heat balance of third experimental zone, the air space of which was sealed. The radiative incident heat was compared with the values calculated by the method used in ASHRAE Handbook of Fundamentals, (see Table 1). In this calculation, the reflection term from the ground was halved in consideration of a small shaded wall which stood four meters from the experimental wall. The experimental and theoretical radiative incidents nearly coincided with each other at the thirteenth hour, as did their totals; however, the experimental radiative incident was generally smaller in the morning and larger in the afternoon. The roof, on which this experimental model was placed, was finished with pebble surfaced asphalt roll roofing on a metal and an insulation plates. Its surface temperature rose in the afternoon, and the re-radiation from the roof surface seems to have had an influence on the radiative incident on the siding surface. For this reason, the experimentally attained radiation incident was used for the following examination of the simulation of heat and air flow in the back space of the sidings of the experimental model. Both sides of the siding were coated with dark brown paint. The plywood surface of the main wall was exposed to outdoor air for five months before the experiment. The absorptance of the four surfaces was assumed to be 0.9. The other thermal constants of the materials used in the experimental model were taken from the ASHRAE Hnadbook of Fundamentals. The physical characters of the air were referred from handbooks of physics, and were evaluated at the mean temperature in the experimental work.

The measured and simulated temperature changes of the surface and air at the centre of the air space in the experimental zone I is compared in (Fig. 4) by using the abscissa as the time axis. The simulated surface temperature change coincides well with the measured surface temperature change. However, the measured air temperature change at all the three measuring points fell in the range between the simulated temperature change at the middle and upper measuring points. The measured air temperature was three to six degrees C higher than the simulated temperature of the corresponding measuring points.

The measured and simulated temperature changes of experimental zone II are compared in (Fig. 5). The measured surface temperature showed one to three degrees C higher values than the simulated values of corresponding times and positions. Measured air temperature at all three heights were about one degree C lower than the simulated temperature for middle and top heights. The measured air temperature change at the lowest measuring point showed two to four degrees C higher values than the simulated temperature change.

The higher air temperature in the experiment may mean :

a) The assumption of laminar flow in the air space is not suitable;
b) Turbulent conditions are caused by the air passage restriction on the frame at the bottom of the air space;
c) The air flow in the space was not as strong as predicted;
d) The heat exchange between the surface and the air in the space is increased by turbulent conditions.

The above points will be discussed in Section 5.

4. RESULTS OF COMPUTER SIMULATION

4.1 Ventilation Effect on Opaque Walls

The performance of the air space ventilation method is examined by loading various conditions of a typical wall structure and orientations into the computer program. The location of a building for this simulation was chosen at a place of latitude 40° north. This enabled the computer simulation to be compared with solar heat gain calculation data presented in the ASHRAE Handbook of Fundamentals. Solar heat gain factors are taken from the July 21 data of Table 6, and Sol-air temperatures are taken from Table 26 of Chapter 22, of the Handbook '72; and they were modified to meet the conditions of heat transfer at siding surface. The temperature and radiative heat incident data, which were used for this simulation, are shown in Table 2.

The temperature distribution in an air space, siding, and external surfaces of a main wall is shown in (Fig. 6); The conditions for this case are : wall height - 2.4 meters, air space thickness - 30 mm, thermal conductance of the main wall - 0.358 watts/m^{2}K (100 mm mineral fiber insulation), and radiative heat incidence - 322 watts/m^2. The aspect ratio of the air space in (Fig. 6) is distorted for illustrative convenience. The surface temperature of the siding is about three degrees C higher than the external surface of the main wall, although the peaks of the isotherm contours deviate to the main wall's side because the air velocity is higher at the siding's side.

The change in air velocity distribution with time is shown in (Fig. 7). The peak air velocity in the air space is displaced from the center of the space to the siding's side as the radiative heat incidence is increased. The air velocity distribution at 11:00 a.m. corresponds to the temperature distribution of (Fig. 6). The air temperature in the siding's surface is higher than that of the main wall's surface. This causes imbalance in buoyancy force through the space, and consequently the air velocity towards the siding is larger than that towards the main wall.

As radiative heat transfer takes place between the siding and main wall surfaces, the temperatures of the siding and of air space side surface of the main wall become higher than that in the air space. This causes reversal of heat flow direction at the air space side surface of the main wall. The heat which is transmitted by radiation to this surface is absorbed by the air stream in the space, and then released to the external environment.

The heat, incident on the siding surface as radiative energy, is traced in Table 3. The conditions of this calculation are the same as that used in (Fig. 6). During the period of 6 a.m. to 6 p.m., the total radiative heat of 1944 watt hours/m^{2}was absorbed by the siding, of which 1726 watt hours/m^2 are dissipated to the outside from the outer surface of the siding by convection and radiation, 169 wH/m^2 are dissipated to the outside by the air change of the air space, 46 wH/m^2 are transmitted into the room through the main wall. When this siding is not applied, 66.9 wH/m^2 are transmitted into the room; this is calculated from the sol-air temperature method. This indicates that the naturally ventilated air space saves 31 % of the cooling load which would othewise be transmitted through the wall of conductance 0.358w/m^2. When the same siding is used, but the back space is sealed, the transmitted heat becomes 64.0 wH/m^2. Employing this value as the reference for the above comparison, the cooling load saving by the ventilation becomes 28 %.

Table 4 shows the average values of air velocity, friction loss, dynamic loss and Reynold's number for the above case. At times of high air velocity, dynamic loss at the holes on framework exceeds 50 % of the total force, and Reynold's number exceeds 400. When the passage restriction is not so tight, dynamic loss is considerably smaller than the friction loss. Air velocity is increased and Reynold's number exceeds the critical value of 1000 in times of high radiative incidence.

Tables 5, 6 and 7 show time-to-time heat transmission into the building through various air space and opening configurations. Table 5 shows the case whereby there is not any obstruction throughout the air passage. The depth of air space is changed from 20 mm to 50 mm.

Of the values of heat transmission, the values with (a) indicate the case whereby the Reynold's number exceeded the critical value. When the depth of air space is 40 mm, the total heat transmission is reduced to 65 % of the heat calculated with an external wall of the same type, except the siding is not applied. As the depth of air space is reduced, the ventilation effect is reduced; the cooling load reduction is also decreased.

Table 6 shows the case when the total opening area of the frame is restricted to 50 % of the sectional area of the enclosed space. A contraction coefficient of 0.6 was applied in considering the flow passage contraction at the openings, the proportion of total heat transmission falls to 71 % of the total heat transmission of the same wall but without siding.

Figure 7 shows the same case, except that the air passage is further restricted to 25 % of the sectional area.

As the depth of an air passage is increased, the effect of ventilation of an air space increases; however, this effect ceases to be of benefit when the depth reaches a certain value.

Table 8 shows the effect of main wall thermal resistance on the total heat transmission of ventilated air space walls. As the thermal resistance of the main wall increases, the effectiveness of the air space ventilation is reduced. However, 20 % reduction is still attainable for a main wall of thermal resistance 5.12 m^2K/w (200 mm mineral fiber insulation) by ventilating the space of the siding.

In Table 9, the effect of emissivity of siding surfaces is examined. The value in the first column is calculated by using 0.9 for the emissivities of two surfaces of the siding and the outer surface of the main wall; this value applies for ordinary surfaces of building materials. In the second column, the emissivity of the back surface of a siding is changed to 0.4; this value corresponds to a metallic paint surface or aggravated metal surface. The third column is calculated for a siding with metallic surfaces on both sides. When the total heat transmission during 6 a.m.through 6 p.m. of each case is compared with the total heat transmission of a wall without this siding, and the emissivity of the external surface of it is 0.9, the effect of a siding and air space ventilation is found to be large.

Tables 10 and 11 show the transmitted heat through east and west oriented walls, respectively.

4.2 Ventilation Effect on Triple-Glazing

A large part of solar gain is caused by fenestration through windows. The thermal performance of a window is very much different from that of an opaque wall. To utilize this simulation method on solar heat gain through a window, several assumptions were made, namely :

a) A triple-glazing window is the study subject. The outermost glass is of heat absorbing type. The middle and inner glasses are clear plates and the space of 12.7 mm between them is completely sealed.

b) The transmitted short-wave radiation through the heat absorbing glass passes completely through the remaining part of the triple glazing. This part directly becomes cooling load.

c) The heat absorbed by the heat absorbing glass produces long wave radiation. The clear plates are completely opaque for this spectral range of radiation.

Under these assumptions, the absorbed heat by the heat absorbing glass is treated, and heat transmission through the glazing is calculated by the simulation program. The short wave transmission is calculated separately. The short-wave transmission and the long-wave transmission compose the total heat gain through a window.

Further assumptions are : the short-wave incidence is absorbed by the heat absorbing glass evenly throughout the thickness, and, both surfaces of the heat absorbing glass is at the same temperature. Here, the heat conductance of the glass is assumed to be large compared with that of the air films on both sides.

The inward long-wave re-radiation from the heat absorbing glass is absorbed completely by the middle glass. The temperature gradient in this glass is assumed to be negligible, because the conductance of the sealed airspace is sufficiently smaller than that of the middle glass.

The same radiative heat incidence as shown in Table 2 was applied. The incident angle was calculated from time to time, and the absorptance and transmittance of a heat-absorbing glass were read from (Fig. 5) of Chapter 22, ASHRAE Handbook of Fundamental 1972.

The trace of radiative heat incidence is shown in Table 12. The simulation subject is a south oriented window with an air space 30 mm between the heat absorbing glass and the middle glass. The total opening area of the air space is 50 % of the sectional area of the air space. The total of direct heat transmission, which is once absorbed by heat absorption glass, is 612 wH/m^2 for the period of 6 a.m. through 6 p.m. The heat transmission through a double-glazing, which has a sealed air space of thickness 12.5 mm, is calculated to be 801 wH/m^2 for the same period. The heat transmission through a triple-glazing (both airspaces are sealed) results in 680 wH/m^2 for the same period. This is 85% of that of unventilated double glazing. The heat transmission 612 wH/m^2 of the ventilated triple glazing corresponds to 76 % of that of an unventilated double glazing (Table 13).

5. DISCUSSION AND CONCLUSION

The simulation of heat and air flows indicated the potential for solar heat gain reduction by passively ventilating a back space of light metal siding. The solar heat gain of a wall of thermal resistance 2.79 m^2K/w, which corresponds to mineral fiber insulation 100 mm, is reduced from 65.5 wH/m^2 to 46.5 wH/m^2 (71 %) by the ventilation of the air space. For a wall of thermal resistance 5.12 m^2K/w, or a wall with 200 mm mineral fiber insulation, the solar heat gain is still reducible from 35.8 wH/m^2 to 28.6 wH/m^2 (80 %) by the ventilation. These reduction rates correspond to additional insulation of 50 mm for these walls.

The computer simulation assumes a laminar flow regime in the air passage, although result comparisons suggest that this may not be the case when incident radiation heat is strong. The computer simulation showed also that when the thichness of an air space exceeds 50 mm, the Reynold's number of the flow exceeds the critical Reynold's number in a strong radiation period. So, in such a case, turbulent flow must be considered. Practically, an entrance passage restriction may cause disturbance in air flow. Consequently, the flow is believed to belong in the turbulent range for more occasions than suggested by the computer simulation prediction.

The following terms may be deduced from the result of the simulation and experimental works.

When the flow belongs to turbulent flow, the ventilation effect of an air space is influenced both positivily and negatively with respect to the computer simulation using laminar flow theory.

If the air flow in an air space belongs to turbulent flow, the heat exchange between a wall surface and the air in the air space becomes considerably greater than the case of laminar flow. This increases the air temperature and consequently, the force to move the air upward. The other difference between laminar and turbulent flows is that the friction loss at a wall surface is increased. If the influence of the positive and negative factors are considered, the estimation of the effect of air space ventilation by a laminar flow theory may not be very much different from actual conditions, as long as the gross heat transmission of a wall is concerned.The high air temperature, which was found in the experimental work, indicates that a potential force exists to motivate the air in a space to flow upward. This ventilation of an air space works effectively in reducing cooling load, when a siding and an air passage is arranged to optimally utilize this natural force of buoyancy.

As the computer simulation based on the laminar flow theory indicated, the ventilation of the back space of siding by natural force has a potential for cooling load reduction on both opaque and transparent building enclosures.

When radiative heat incident is nil or little, slight air flow is caused by the heat, which is supplied to an air space through the insulated main wall. The direction of this air flow is downward in a cooling season, and is upward in a heating season. This may reduce the thermal performance of an air space ventilated wall in summer nights and in winter. This effect of having the openings in other seasons than summer remains to be investigated. The performance analysis method to employ this technique effectively is under development by the authors.

The air space temperature exceeds often 70 °C, when it is not ventilated.

Such a high temperature accelerate the aging of organic insulation materials. The ventilation of back space of a siding is effective to prevent the aggravation of insulation effect.

From the above results, the effect of air space ventilation seems significant for cooling load reduction of buildings. The method is attractive also because it is passive.

REFERENCES

1. Vennard, J.K., Elementary Fluid Mechanics, John Willy and Sons, Inc., New York, 1962
2. Kaufmann, W., Fluid Mechanics, McGraw-Hill Book Co., Inc., New York, 1963
3. Grober, H., Erk, S. and Grigull, U., Fundamentals of Heat Transfer, McGraw-Hill Book Co., Inc., New York, 1961
4. ASHRAE Handbook of Fundamentals, American Society of Heating, Refrigerating and Air-Conditioning Engineers, New York, 1972

Table 1. Radiation Incidence on Experimental Model, August 17, 1979

Time	a) Calculated from heat balance of sealed section w/m^2	b) Calculated by ASHRAE method w/m^2	a) - b) w/m^2
10	283	520	-237
11	404	601	-187
12	512	629	-117
13	612	601	+ 20
14	680	520	+160
15	545	392	+153
16	377	240	+137
17	288	74	+214
Total *	3,702 wH/m^2	3,577 wH/m^2	+133 wH/m^2 (+3.6%)

*Total of 6 hours

Table 2. Temprature and Radiation Incidence data for 40° North Latitude on July 21

Time	Air Temp. °C	Radiation w/m^2 East Wall	South Wall	West Wall	Sol air temprature °C East	South	West
6	23.3	432	32	32	42,8	24.4	24.4
7	23.9	643	63	60	52.5	26.7	26.7
8	25.0	688	91	82	55.8	30.0	28.6
9	26.7	611	164	98	55.0	36.9	31.1
10	28.3	460	252	110	50.8	42.8	33.3
11	30.6	255	322	117	45.0	48.1	35.8
12	32.3	129	344	129	32.1	50.6	38.1
13	33.9	117	322	255	39.2	51.4	48.3
14	39.4	110	252	460	39.4	48.9	56.9
15	35.0	98	164	611	39.4	45.3	63.3
16	34.4	82	90	681	38.1	39.4	65.3
17	33.9	60	63	643	36.7	36.7	62.5
18	32.8	32	32	432	33.9	33.9	52.5

Converted from table 4 and 26 of Ch. 22, ASHRAE Handbook of Fundamentals,1972.

Table 3. Trace of Radiative Heat Incidence

South wall, air space thickness 30mm
Proportion of total opening area 50%
Height of air space 2.4 m

Latitude 40° N
July 21
Indoor air temp. 24°C

Time	Air Temperature	Absorbed radiation w/m^2	Dissipation from outer surface w/m^2	Dissipation by air change w/m^2	Transmitted into room w/m^2
6	23.3	28.8	27.4	1.2	.1
7	23.9	56.7	52.7	3.4	.6
8	25.0	81.7	75.1	5.6	1.3
9	26.7	147.6	132.8	12.2	2.5
10	28.3	226.8	201.5	21.3	3.7
11	30.6	289.8	255.5	28.8	5.1
12	32.2	309.6	272.3	31.0	5.8
13	33.9	289.8	255.1	28.1	6.1
14	34.4	226.8	200.6	20.2	5.7
15	35.0	147.6	131.3	11.1	5.2
16	34.4	81.0	72.2	4.4	4.3
17	33.9	56.7	59.4	2.4	3.9
18	32.8	28.8	25.0	0.6	3.2
Total* wh/m^2		1944.0	1725.7	169.4	45.9

*Total ; total of 12 hours, 6 a.m. through 6 p.m.
Thermal conductance of main wall 0.358 w/m^2K

Table 4. Characteristics of Air Flow

40°N, July 21, Conductance of wall 0.358 W/m K
South wall, depth of air space 30mm height of air space 2.4 m
Emissivities of surfaces 0.9, Proportion of total opening area 50%
Indoor air temperature 24°C

Time	Average Velocity m/s	Friction Loss N/m2	Dynamics Loss N/m2	Reynold's No.
6	0.06	0.066	.029	129
7	0.100	0.102	.064	189
8	0.121	0.128	.094	228
9	0.164	0.186	.169	304
10	0.201	0.241	.255	369
11	0.224	0.287	.318	408
12	0.231	0.298	.336	416
13	0.222	0.282	.312	400
14	0.196	0.237	.244	355
15	0.157	0.175	.156	283
16	0.111	0.114	.078	202
17	0.088	0.087	.049	161
18	0.052	0.049	.017	95

Table 5. Performance of Ventilated Air Space Wall

Time	Air Space Thickness mm				
	10	20	30	40	50
	Heat Transmission into room w/m^2				
6	.2	.2	.1	.1	.1
7	.8	.7	.6	.6	.5
8	1.5	1.3	1.2	1.1	1.1
9	2.9	2.5	2.3	2.3	2.3
10	4.5	3.8	3.5	3.5	3.5(a)
11	6.0	5.1	4.8	4.7	4.7(a)
12	6.8	5.8	5.5	5.4	5.4(a)
13	7.1	6.2	5.9	5.8	5.8(a)
14	6.5	5.8	5.5	5.5	5.5(a)
15	5.6	5.3	5.3	5.0	5.0
16	4.5	4.4	4.2	4.2	4.2
17	4.0	3.9	3.8	3.8	3.8
18	2.3	3.2	3.2	3.2	3.2
Total*	52.0	46.5	44.0	43.6	43.5 wH/m^2
Proportion to a)**	78%	70%	66%	65%	65%

Latitude 40° N — Date ; July 21
South wall — Indoor air temperature ; 24°C
Height of air space 2.4 m — Thermal conductance of main wall 0.358 w/m^{2}K
Proportion of total opening area 100 %
* Total ; total of 12 hours 6 a.m. through 6 p.m.
** Case a) ; heat transmission of the same wall, but without siding calculated using Sol-air temperature

Table 6. Performance of Ventilated Air Space Wall

Proportion of Opening - 50%

Time	Depth of air space in mm							
	10	20	30	40	50	65	80	100
	Heat transmission into room w/m^2							
6	.2	.2	.1	.1	.1	.1	.1	.1
7	.8	.7	.6	.6	.6	.6	.6	.6
8	1.5	1.4	1.2	1.2	1.2	1.2	1.2	1.2
9	2.9	2.6	2.4	2.4	2.4	2.4	2.4	2.4
10	4.5	4.0	3.7	3.7	3.6	3.6	3.6	3.7 (a)
11	6.0	5.3	4.0	4.0	5.0	5.0	5.0	5.0 (a)
12	6.8	6.1	4.7	4.7	5.7	5.7	5.7	5.7 (a)
13	7.1	6.4	6.1	6.1	6.0	6.0	6.1	6.1 (a)
14	6.5	6.0	5.7	5.7	5.6	5.6	5.6	5.6 (a)
15	5.6	5.3	5.2	5.1	5.1	5.1	5.1	5.1
16	4.5	4.4	4.3	4.3	4.2	4.2	4.2	4.2
17	4.0	3.9	3.8	3.8	3.8	3.8	3.8	3.8
18	3.3	3.2	3.2	3.2	3.2	3.2	3.2	3.2
Total*	53.7	47.8	45.8	46.9	46.5	46.5	46.6	46.7 wH/m^2
Proportion to a**	.82	.75	.72	.71	.71	.71	.71	.71

(a) shows the case when Reynold's number exceeds 1000
Total* ; Total for 12 hour of 6 a.m. through 6 p.m.

Latitude 40° N July 21 — South wall — Indoor air temp. 24°C
Height of air space 2.4m — Thermal conductance of main wall 0.358w/m^{2}K
a**; heat transmission of the same wall, but without siding calculated using Sol-air temperature

Table 7. Performance of Ventilated Air Space Wall

Latitude 40° N July 21 South wall Indoor temp. 24°C
Proportion of opening - 25% Height of air space 2.4 m

Depth of space in mm

Time	10	20	30	40	50	65	80	100
	Heat transmission into room in W/m2							
6	.2	.2	.1	.1	.1	.1	.1	.1
7	.8	.7	.7	.6	.6	.6	.6	.6
8	1.5	1.4	1.3	1.3	1.3	1.2	1.2	1.2
9	2.9	2.7	2.6	2.5	2.5	2.5	2.5	2.5
10	4.5	4.2	4.0	3.9	3.8	3.8	3.8	3.8
11	6.1	5.6	5.3	5.2	5.2	5.2	5.2(a)	5.2(a)
12	6.9	6.3	6.1	6.0	5.9	5.9	5.9(a)	5.9(a)
13	7.2	6.7	6.4	6.3	6.3	6.3	6.2(a)	6.2(a)
14	6.5	6.1	5.9	5.9	5.8	5.8	5.8	5.8(a)
15	5.6	5.4	5.3	5.2	5.2	5.2	5.2	5.2(a)
16	4.5	4.4	4.2	4.3	4.3	4.3	4.3	4.3
17	4.0	3.9	3.9	3.9	3.9	3.8	3.8	3.8
18	3.3	3.2	3.2	3.2	3.2	3.2	3.2	3.2
Total*	54.0	50.8	49.1	48.4	48.1	47.8	47.8	47.8 wH/m^2
Proportion to a**	.82	.77	.75	.74	.73	.73	.73	.73

Thermal conductance of main wall 0.358 w/m^{2}K
Total* ; total of 12 hour 6 a.m. through 6 p.m.
a** ; Heat transmission of the same wall, but without siding calculated using Sol-air temperature

Table 8. Effect of Thermal Resistances of Main Walls on Heat Transmission into a Room
Proportion of total opening area -50%

Time	Thermal resistance of main wall in m^2 K/w 1.56	2.79	5.12
	Heat transmission into room in w/m^2		
6	.2	.1	.1
7	1.0	.6	.4
8	2.0	1.2	.8
9	4.0	2.4	1.5
10	6.1	3.6	2.3
11	8.3	5.0	3.2
12	9.5	5.7	3.6
13	10.1	6.0	3.8
14	9.4	5.6	2.6
15	8.5	5.1	3.2
16	7.0	4.2	2.7
17	6.4	3.8	2.4
18	5.3	3.2	2.0
Total * wH/m^2	75.1	46.5	28.6 wH/m^2
Without ventilation	110.4	64.5	35.8 wH/m^2
Proportion	.68	.71	.80

Latitude 40° N July 21 South wall Indoor temp. 24°C
Thickness of air space 50 mm Height of air space 2.4 m
Thermal concuctance of main wall 0.358 w/m^{2}K
Total* ; total of 12 hours 6 a.m. through 6 p.m.

Table 9. Effect of Emmissivity of Siding Surfaces on The Heat Transmission into a Room

Latitude 40° N July 21 South wall Indoor temp. 24°C
Air space thickness - 50mm Air space height 2.4 m
Proportion of total opening area - 25%

Time	Position	Emissivity		
	Siding outer surface	0.9	0.9	0.4
	Siding inner surface	0.9	0.4	0.4
		Heat transmission into room in w/m^2		
6		.1	.1	-0.1
7		.6	.5	.2
8		1.3	1.1	.7
9		2.5	2.2	1.5
10		3.8	3.4	2.0
11		5.2	4.6	3.3
12		5.9	5.3	3.9
13		6.3	5.7	4.3
14		5.8	5.3	4.2
15		5.2	4.8	4.1
16		4.3	4.0	3.6
17		3.9	3.7	3.3
18		3.2	3.0	2.8
Total * wH/m^2		48.1	42.2	32.8
Proportion of case a*		.72	.63	.49

Thermal conductance of main wall 0.358 w/m^2K
Total* ; total of 12 hours 6 a.m. through 6 p.m.
case a* ; heat transmission of the same wall, but without siding calculated using Sol-air temperature

Table 10 . Heat Flow of East Wall

Time	Thickness of air space in mm		
	30	40	50
	Heat transmission into room in w/m^2		
6	3.5	3.5	3.4
7	5.4	5.3	5.3
8	6.0	5.9	5.9
9	6.1	6.0	5.9
10	5.4	5.3	5.3
11	4.5	4.4	4.4
12	3.9	3.9	3.9
13	4.4	4.3	4.3
14	4.5	4.4	4.4
15	4.6	4.5	4.5
16	4.2	4.2	4.2
17	3.8	3.8	3.8
18	3.2	3.2	3.2
Total* WH/m^2	56.1	55.4	55.2
Proportion to case a**	.69	.68	.68

Proportion of total opening area - 50%

Air space height 2.4 m
Latitude 40° N July 21 Indoor temp. 24°C
Thermal conductance of main wall o.358 w/m^2K
Total* ; total of 12 hours 6 a.m. through 6 p.m.
case a** ; heat transmission of the same wall, but without siding calculated using Sol-air temperature

Table 11. Heat Flow of West Wall

Time	Thickness of air space in mm		
	30	40	50
	Heat transmission into room in w/m^2		
6	0.1	0.1	0.1
7	0.6	0.6	0.6
8	1.2	1.1	1.1
9	1.9	1.8	1.8
10	2.5	2.5	2.4
11	3.3	3.3	3.2
12	3.9	3.9	3.9
13	5.6	5.5	5.5
14	7.4	7.3	7.3
15	8.8	8.7	8.7
16	9.1	9.0	9.0
17	8.7	8.6	8.6
18	6.7	6.6	6.6
Total*	56.4	55.7	55.5 wH/m^2
Proportion to a**	.69	.68	.68

Proportion of total opening area 50%
Air space height 2.4 m
Latitude 40° N July 21 Indoor temp. 24°C
Thermal conductance of main wall 0.358 w/m^{2}K
Total* ; total of 12 hours 6 a.m. through 6 p.m.
case a** ; heat transmission of the same wall, but without siding calculated using Sol-air temperature

Table 12. Heat Balance of Ventilated Triple Window

South Window
Air space thickness - 30mm
Proportion of total opening area 50%

Time	Transmitted to room directly	Absorbed by First glass	Dissipated from outer Surface	Dissipated by air change	Transmitted to room indirectly	Total direct and indirect
6	3.2 w/m^2	3.2 w/m^2	4.1 w/m2	0.1 w/m^2	-1.0 w/m^2	2.2 w/m2
7	4.0	4.0	3.8	0.0	0.1	4.1
8	4.6	4.6	2.4	0.0	2.2	6.8
9	16.4	65.6	53.7	2.2	9.6	26.0
10	50.4	121.0	98.9	5.8	16.3	66.7
11	80.5	161.0	129.6	8.2	23.1	103.6
12	90.9	178.9	142.5	9.0	27.3	118.2
13	80.5	161.0	125.0	6.5	29.4	109.9
14	50.4	121.0	90.0	3.2	27.8	78.2
15	16.4	65.6	40.4	0.2	25.0	41.4
16	4.6	4.6	-14.5	0.0	19.1	23.7
17	4.0	4.0	-14.1	0.0	18.1	22.1
18	3.2	3.2	-12.9	0.0	16.1	19.3
Total wH/m^2 (6 a.m.-6 p.m.)	405.9	894.5	653.3	35.2	205.6	611.5
Proportion to case a*						0.76

Case a* ; heat transmission of unventilated double glazing window

Table 13. performance of Ventilated Triple Glazing

South Window
Proportion of total opening area - 50%

Time	Air Space Thickness			
	30mm	40mm	50mm	
6	-1.0w/m2	-1.0w/m^2	-1.0w/m^2	
7	.1	.1	.1	
8	2.2	2.1	2.1	
9	9.6	9.5	9.4	
10	16.3	16.0	15.8	
11	23.1	22.8	22.6	
12	27.3	26.9	26.8	
13	29.4	29.0	28.8	
14	27.8	27.4	27.2	
15	25.0	24.8	24.6	
16	19.1	18.9	18.8	
17	18.1	18.0	17.9	
18	16.1	16.0	15.9	
Total indirect	205.6	203.0	201.7	wH/m^2
Total direct	405.9	405.9	405.9	wH/m^2
Total*	611.5	608.9	607.6	wH/m^2
Proportion to unventilated double glazing	.76	.76	.76	

Total* ; total of 12 hours 6 a.m. through 6 p.m.

Table 14. Performance of Ventilated Triple Glazing Heat Transmition into Room
South Window
Proportion of total opening area - 50%

Time	Air Space Thickness		
	30mm	40mm	50mm
6	-1.0w/m^2	-1.0w/m^2	-1.0w/m^2
7	.1	.1	.1
8	2.2	2.1	2.1
9	9.8	9.6	9.5
10	16.6	16.3	16.2
11	23.6	23.2	23.0
12	27.8	27.4	27.1
13	29.8	29.3	29.1
14	27.9	27.6	27.4
15	25.0	24.8	24.6
16	19.1	18.9	18.8
17	18.1	18.0	17.9
18	16.1	16.0	15.9
Total* of			
Indirect	207.6	204.8	203.3 wH/m^2
Direct	405.9	405.9	405.9 wH/m^2
Total*	613.5	610.7	609.2 wH/m^2
Proportion to unventilated double glazing	.77	.76	.76

Total* ; total of 12 hours 6 a.m. throught 6 p.m.

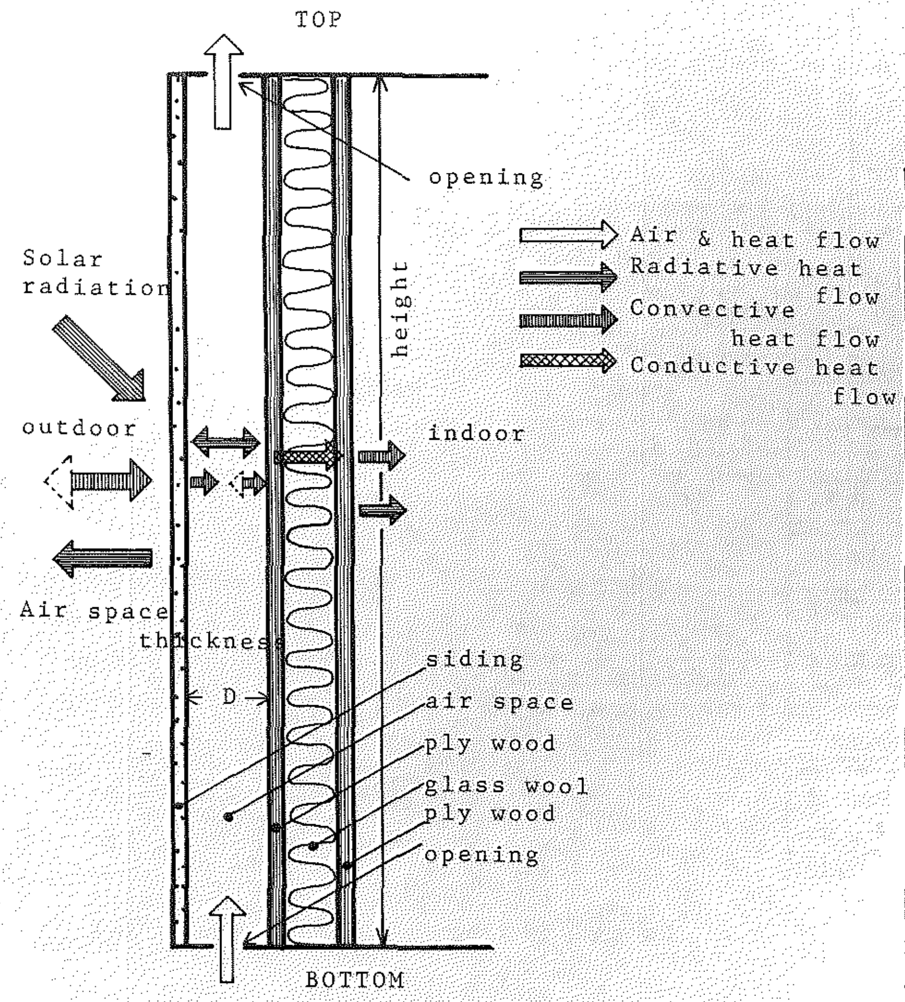

Fig. 1 Model of Gross Heat and Air Flows at a Wall (Vertical Section)

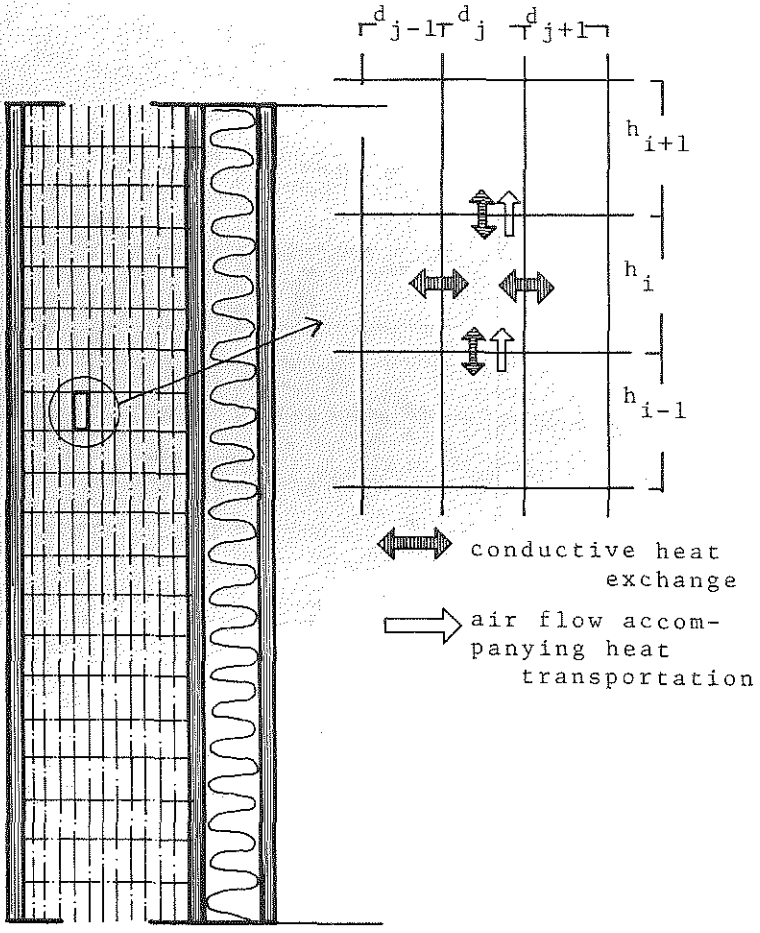

Fig. 2 Division of Air Space into Finite Control Spaces and Heat Exchange at One of the Finite Control Spaces

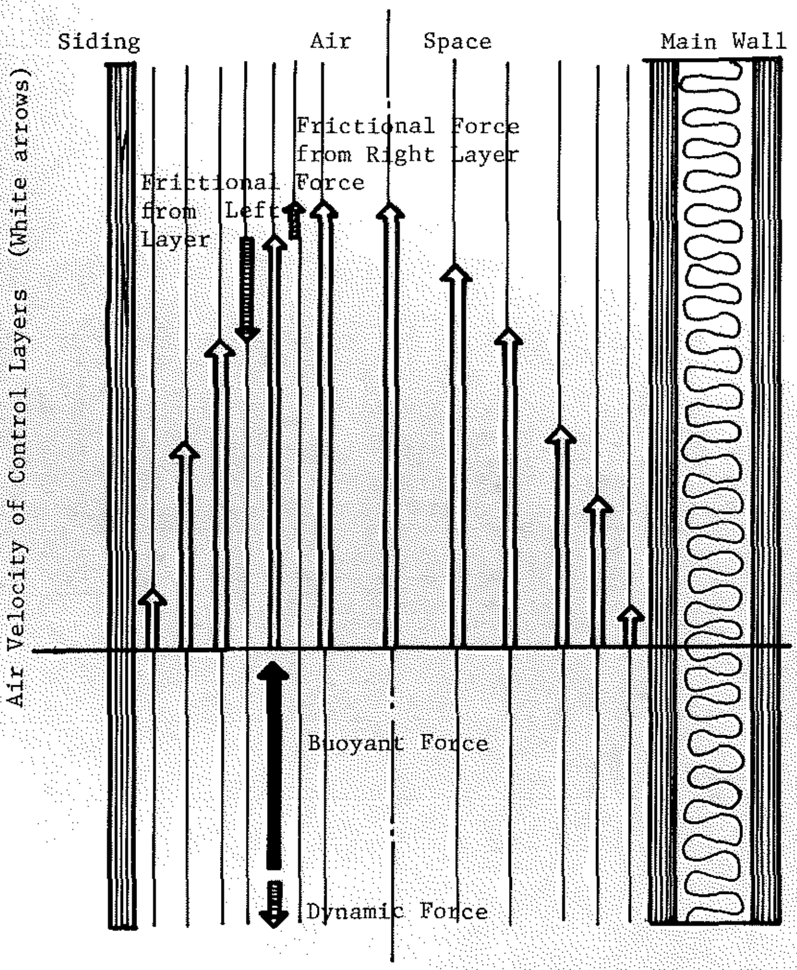

Fig. 3 Balance of Forces of a Control Layer

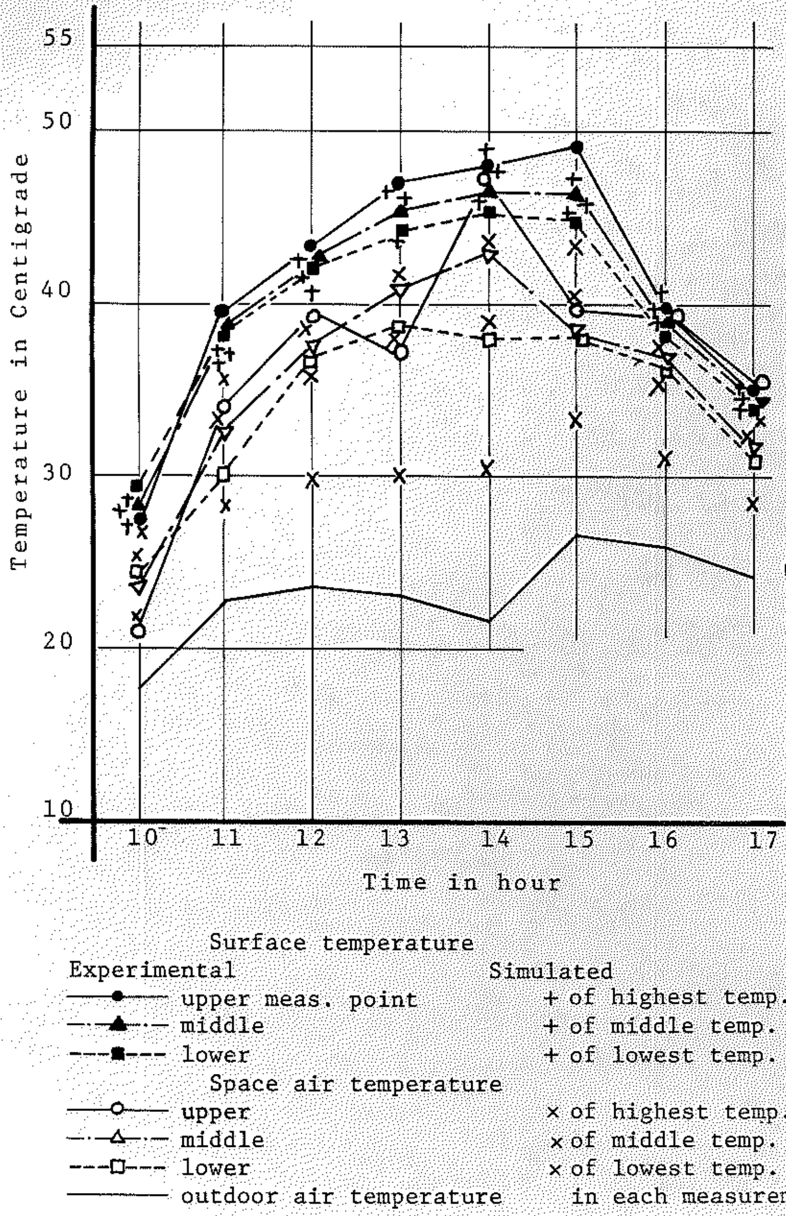

Fig. 4 Surface and Air Temperature Change of Experimental Zone I
Proportion of Total Opening area to Sectional Area of Air Space - 19%

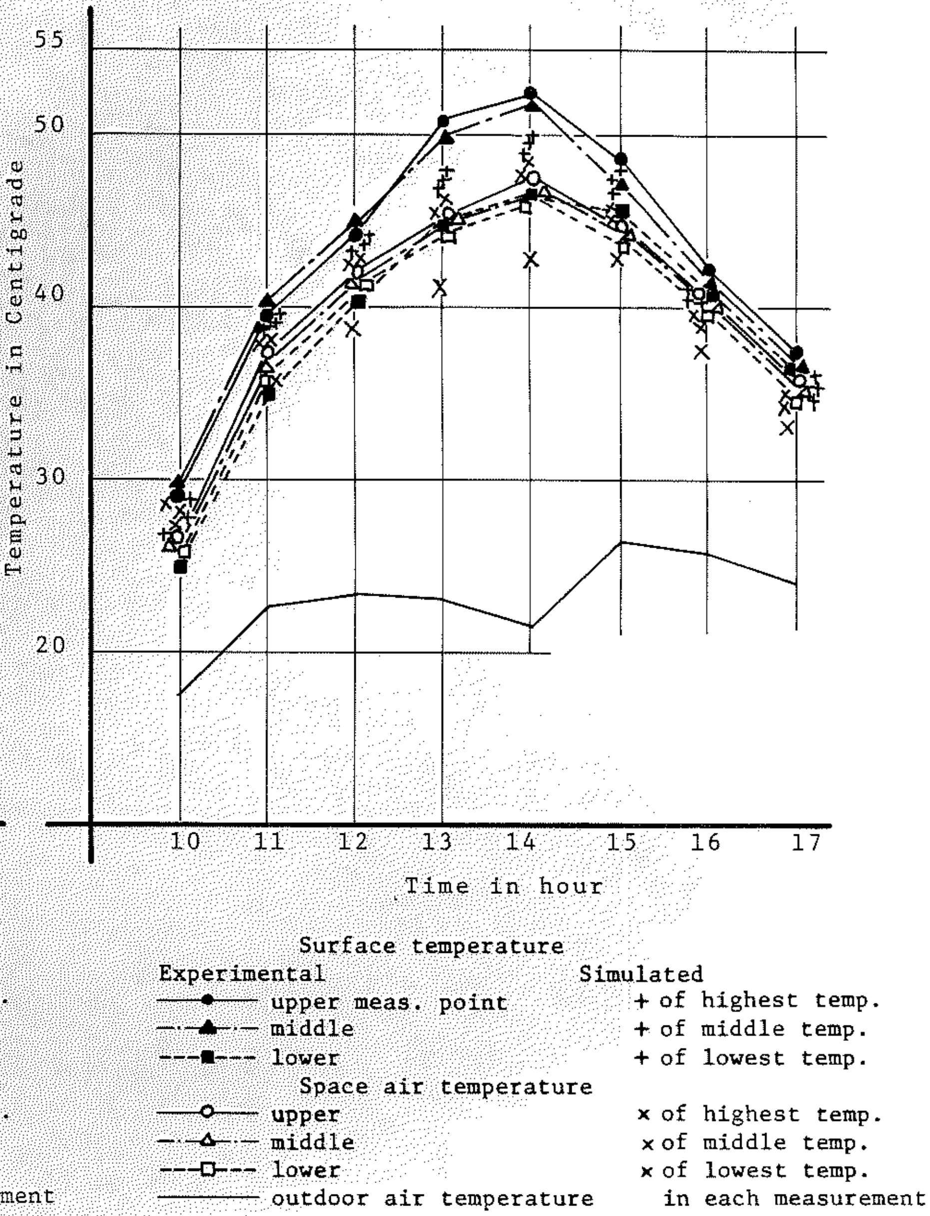

Fig. 5 Surface and Air Temperature Changes of Experimental Zone II
Proportion of Total Opening area to Sectional Area of Air Space - 4%

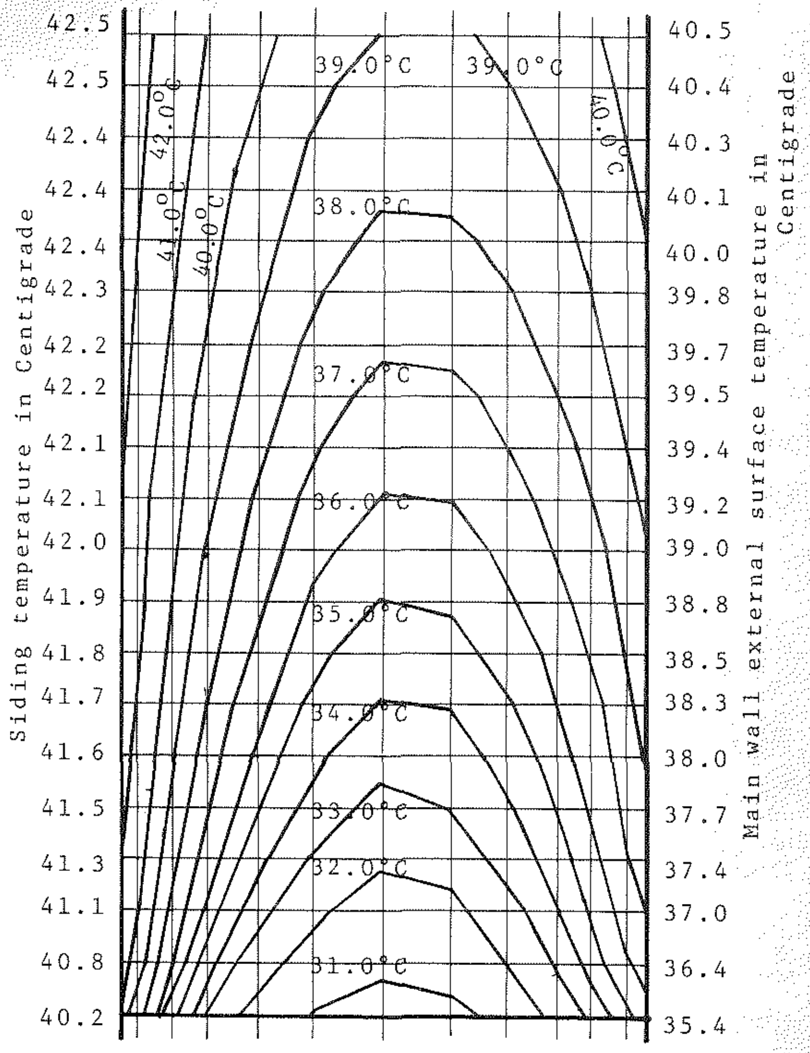

Fig. 6 - Temperature Distribution in Air space and Surfaces (inflow air temperature 30.6°C)

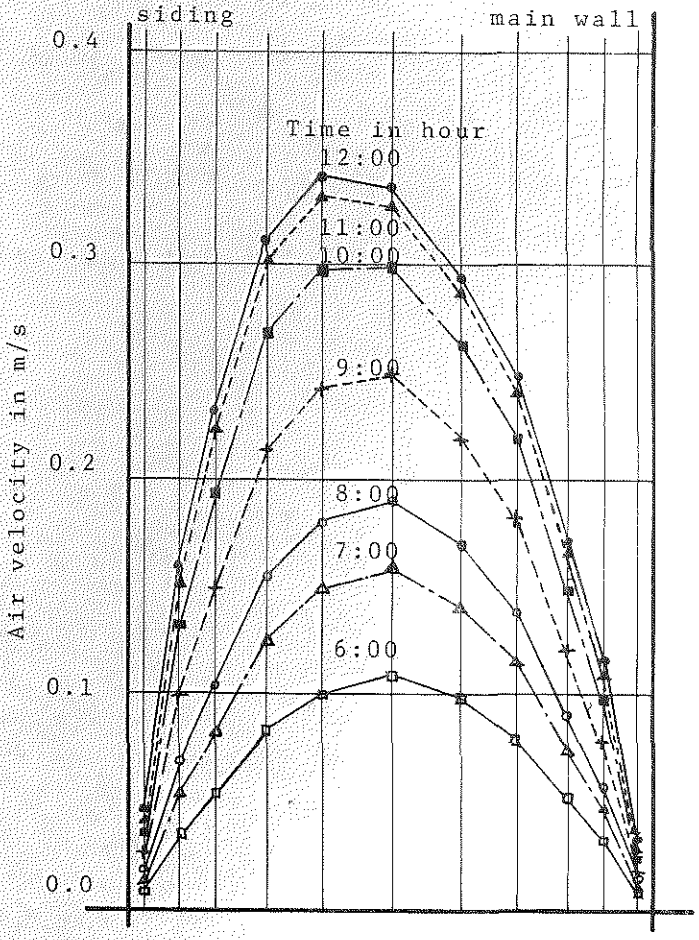

Fig. 7 - Air Velocity Distribution in Air Space